Preprint PFC/JA-80-28

NUMERICAL SIMULATION OF OSCILLATING MAGNETRONS

A. Palevsky and G. Bekefi

Massachusetts Institute of Technology
Cambridge, Massachusetts 02139

and

A. T. Drobot

Science Applications, Inc.
McLean, Virginia, 22101

December 1980

NUMERICAL SIMULATION OF OSCILLATING MAGNETRONS*

A. Palevsky and G. Bekefi

Department of Physics and Research Laboratory of Electronics

Massachusetts Institute of Technology

Cambridge, Massachusetts, 02139

and

A. T. Drobot

Science Applications, Inc.

McLean, Virginia, 22101

ABSTRACT

The temporal evolution of the current, voltage and rf fields in magnetron-type devices has been simulated numerically by a two-dimensional, electromagnetic, fully relativistic particle-in-cell code. The simulation allows for the complete geometry of the anode vane structure, space-charge limited cathode emission, and the external power source. The code has been applied to magnetrons operating in the relativistic energy regime.

Unprecedented rf powers (~300MW to ~3GW) have been achieved in relativistic magnetrons[1-9] operating at voltages from several hundred kilovolts to 1MV, and drawing kiloamperes of current from field emission cathodes. These impressive results have reawakened an interest to better understand the interaction of the electromagnetic field and the dense space charge cloud in magnetron-type devices. Numerous attempts have been made over a span of forty years[10-14] to calculate self-consistently the rf fields under the large signal conditions prevalent in the magnetron, and from these to predict the current, voltage, microwave power and efficiency. Since these studies are based on certain assumed steady state configurations, they give but a qualitative understanding of the phenomena. At best, they yield magnetron scaling laws[10] useful to microwave tube designers. This Letter describes a self-consistent numerical simulation which addresses itself to those questions that have eluded analytic techniques. The simulation is a two-dimensional, electromagnetic, fully relativistic particle-in-cell[15,16,17] code. It includes the complete geometry of the vane resonators embedded in the anode block, rf loading of the resonators, space-charge limited emission from the cathode, and the external voltage source of finite impedance. The simulation is also applicable to smooth bore magnetrons[18,19,20] and to the study of magnetically insulated high-voltage transmission systems.[21] The code embodies several major improvements over an earlier magnetron simulation[22] which was electrostatic (in the moving wave frame), and which did not treat the anode geometry in detail.

Our simulation has been applied to a 54 vane inverted relativistic magnetron[9] operating at a voltage of ~300kV and a magnetic

field of ~0.17T. Because of the large radius of curvature of the anode block, it was possible to approximate the cylindrical device by a planar analog, two vanes of which are shown to scale in Fig. 1. In the simulation, the two-vane structure was represented on a 32×32 mesh, and the fields and particle positions were integrated forward in time with successive time steps of 2×10^{-12}s. Each of the simulation particles contained 2×10^{10} electrons. At time t=0, a voltage ramp was applied to the cathode-anode gap with a rise time of 3×10^{-9}s (~15 cyclotron periods) reaching a maximum value of 600kV. A series resistance of 375Ω was placed in the external circuit.

Figure 1 shows the particle distribution at two instances of time. At 5ns, the magnetron is essentially in its "preoscillation"[23] stage. No particles reach the anode and the diode is said to be "magnetically insulated". Most particles are confined to a region which extends from the surface of the cathode to the top of the theoretical space charge layer (shown by the horizontal dashed line) above which no particles could in principle reside if steady state, equilibrium conditions were reached in an adiabatic manner.[20] That particles do find their way above this layer is indicative of the fact that the space charge cloud is perturbed by transit time effects even in the preoscillation stage of development. Indeed, the absence[24,25] of a sharp space charge boundary and the presence of turbulent oscillations[20,26] have been observed in a variety of experiments. At 15ns the magnetron is in its fully oscillating state. This is characterized by the presence of rotating space charge spokes,[10,12,22] one of which is seen in the lower half of Fig. 1. Now, despite the strong perpendicular magnetic field,

particles can cross from cathode to anode under the influence of the large rf fields which exist both in the gap and in the vane resonators. The change in thickness of the space charge cloud in going from 5ns to 15ns is due to a fall in the magnetron voltage.

Our numerical simulation also yields a complete space-time history of the particle momenta. Figure 2 illustrates the spatial distribution of the momentum components parallel to the cathode surface during the preoscillation stage (5ns), and during the fully oscillating stage (15ns). The vertical dashed lines once again delineate the "classical" boundary of the space charge cloud, and the horizontal dot-dashed lines give the corresponding values of the momenta of these boundary particles, as calculated for Brillouin equilibrium. We see from the top diagram of Fig. 2 that at early times (5ns), the momentum is strongly sheared, rising almost linearly from zero at the cathode to its maximum value at the space charge boundary. This behavior is in good agreement with predictions of steady state, cold fluid theory.[27] Of course, the spread of momenta about the average, suggesting finite temperature effects, is not predicted by the fluid model. At late times (15ns), particles residing within the space charge cloud continue to have an approximately linear momentum versus position behavior. However, particles near the top of the space charge layer are scattered by the strong, synchronous rf fields that exist there. For efficient wave-particle interaction to occur, near synchronism must exist between the particle velocity and the phase velocity of the slow electromagnetic wave traveling along the structure. We find that at 15ns, synchronism occurs for particles residing at the very top of the Brillouin layer, traveling at a velocity of

1.13×10^8 m/s. Lower lying particles are not synchronous, and here the rf fields, though strong, have little effect beyond possibly causing mild particle heating. We note that the observed synchronism of the uppermost layer is a statement of the fact that our fully oscillating magnetron operates exactly at the Buneman-Hartree[7,28] oscillation threshold.

A study of the spatial distribution of the vertical particle momenta sheds light on a long standing controversy between two steady-state models. Is the electron flow laminar, parallel to the cathode, as proponents[29-34] of Brillouin or "parapotential" flow would have it? Or are the electron paths cycloidal, beginning and ending on the cathode, as Gabor and others have claimed?[35-40] Results from our simulation show that the flow is mixed: at any given time, there is a class of particles whose motion is largely laminar, and a class of particles whose motion is largely cycloidal, together with particles exhibiting a gradual transition between these two states. Cold fluid theory does not predict the existence of the in-between type of motions.

The temporal buildup of the current, voltage, and the rf fields is illustrated in Fig. 3. The amplitude of the rf field in the expected mode of operation (the π mode[10] in which fields in adjacent vanes are 180° out of phase) was initialized in the computer code. This "priming" was done in order to reduce computer costs, since it was not known a priori how long it would take the signal to grow from noise (as it does in an actual magnetron). The current drawn during the first three nanoseconds is due mainly to the capacitive charging of the device which has initially a very large impedance. In the time interval from ~5ns to ~8ns,

the current rises, the voltage falls, and magnetic insulation is broken; the rf fields grow exponentially. This short time interval, less than 10 cyclotron periods long delineates the "small signal" stage of operation. From 8 to 13ns, the current and the fields increase more slowly and beyond ~13ns the system settles to an approximate steady state. At this time, 8% of the total power from the external circuit appears as microwave power deposited in the rf loads which terminate the vane resonators. The remainder of the power is deposited in the form of heat in the anode (74%), and through back bombardment[10,23] of the cathode (18%). The rf fields are high both in the vanes and in the gap, and are of the order of or greater than the dc field. Consequently, there is strong coupling between the way particles are created at the cathode (the emission law), and the rf fields that exist there. For example, at 15ns, the ratio V_{rf}/V_{dc}=1.8 where V_{rf} is the rf electric field integrated over the length of the vane resonator and V_{dc} is the dc voltage across the anode-cathode gap. This high value of the ratio V_{rf}/V_{dc} is undesirable from the point of view of a practical device, and is probably due in part to the high Q we have chosen for the vane resonators (Q=550). Lowering the Q may also improve the efficiency of the device. However, no attempt has yet been made to optimize the magnetron by varying parameters in the simulation.

We have also begun a particle simulation (in r, θ coordinates) of a compact six vane magnetron[1,2,3] operating at a frequency of 4.6GHz and capable of delivering[7] an average power of ~400MW at a voltage of 350kV and[41] ~900MW at a voltage of 1MV. This unusual magnetron is characterized by a very small anode-cathode gap size

(0.55cm), which has the tendency to short out the tangential rf electric fields. Consequently,[7] the device operates in the 2π mode, in which the rf fields in adjacent vanes are in phase rather than being out of phase as is the case in conventional magnetrons.

In conclusion, then, we have presented some initial results from our magnetron simulation. To achieve these results several innovations were incorporated in the code. The first was the inclusion of the complete anode vane structure in the treatment of the applied and rf fields. Previous simulations[22] modeled only the anode-cathode gap and used L-C lumped circuit models for the resonators. Second, rf loads were included in the resonators to allow for the adjustment of the cavity Q and load symmetry. Third, the cathode was modeled by an algorithm that produces local space-charge limited emission. This was accomplished by placing enough new particles into the simulation along the cathode at every time step to reduce the local perpendicular electric field to zero. The technique[42] leads to the correct relativistic form of the Child-Langmuir law[43] for the case of smooth surfaces, and zero insulating magnetic fields. The advantage of this algorithm is that it performs correctly for irregular geometry and in the presence of the large dc magnetic field and rf fields. The technique has been previously used only in electrostatic codes.

Finally, the power supply for the magnetron was included in the simulation, by coupling a lumped circuit model for the generator to the particle-in-cell code. The circuit consisted of a voltage source with a series resistor and inductor, (but this could easily be extended to include more components). A time integration of the circuit parameters and of the voltage across the

anode-cathode gap generated the circuit current. This current appeared as a displacement current in the simulation and generated an electric field there. However, in the presence of strong rf fields the conventional definition of voltages, $V=\int\vec{E}\cdot d\vec{\ell}$, is not appropriate. A more general definition was therefore invented[44] which reduces to the conventional result for purely electrostatic fields and also leads to energy and charge conservation in the combined lumped circuit and 2-d particle-in-cell simulation.

ACKNOWLEDGMENTS

This work was supported in part by the U.S. Air Force Office of Scientific Research under Grant AFOSR 77-3143 and in part by the National Science Foundation under Grant ENG 79-07047.

REFERENCES

1. G. Bekefi and T.J. Orzechowski, Phys. Rev. Lett. 37, 379 (1976).

2. G. Bekefi and T.J. Orzechowski, Bull. Am. Phys. Soc. 21, 571 (1976).

3. T.J. Orzechowski, G. Bekefi, A. Palevsky, W.M. Black, S.P. Schlesinger, V.L. Granatstein, and R.K. Parker, Bull. Am. Phys. Soc. 21, 1112 (1976).

4. A. Palevsky, R.J. Hansman, Jr., and G. Bekefi, Bull. Am. Phys. Soc. 22, 648 (1977).

5. N.F. Kovalev, B.D. Kol'chugin, V.E. Nechaev, M.M. Ofitserov, E.I. Soluyanov, and M.I. Fuks, Pis'ma Zh. Tekh. Fiz. 3, 1048 (1977) [Sov. Tech. Phys. Lett. 3, 430 (1977)]; also V.E. Nechaev, M.I. Petelin, and M.I. Fuks, Pis'ma Zh. Tekh. Fiz. 3, 763 (1977) [Sov. Tech. Phys. Lett. 3, 310 (1977)].

6. A.N. Didenko, A.S. Sulakshin, G.P. Fomenko, Yu. G.Shtein and Yu. G. Yushkov, Pis'ma Zh. Tekh. Fiz. 4, 10 (1978) [Sov. Tech. Phys. Lett. 4, 3 (1978)].

7. A. Palevsky and G. Bekefi, Phys. Fluids 22, 986 (1979).

8. G. Craig, J. Pettibone, and D. Ensley, Proc. IEEE International Conference on Plasma Science (IEEE Cat. No. 79CH1410-ONPS) p.44 (1979).

9. R.K. Parker, W.M. Black, R.A.Tobin, and G. Farney, Proc. IEEE International Conference on Plasma Science (IEEE Cat. No. 79CH1410-ONPS) p.44 (1979); I.E.D.M. Tech. Digest, 175 (1979).

10. "Microwave Magnetrons", edited by G. B. Collins (McGraw-Hill, New York, 1948).

11. O. Buneman, J. Electron Contr. No. 1, p. 1, July 1957.

12. "Crossed-Field Microwave Devices", edited by E. Okress (Academic, New York, 1961).

13. P.L. Kapitsa, "High Power Microwave Electronics" (Pergamon, New York, 1964).

14. J.R.M. Vaughan, IEEE Trans. Electon Devices ED-20, 818 (1973).

15. C.K. Birdsall, A.B. Landgon, H. Okuda, in "Methods of Computational Physics", edited by B. Adler, S. Fernbach, and M. Rotenberg (Academic Press, New York 1970), 9, pp. 241-258.

16. J.P. Boris, in "Proceedings of the Fourth Conference on Numerical Simulation of Plasmas", edited by J.P. Boris and R.A. Shanny (Stock 0851 0059, U.S. Govt. Printing Off., Washington, D.C., 1971), pp.3-67.

17. A.B. Langdon and B.F. Lasinski, in "Methods of Computational Physics", edited by B. Adler, S. Fernbach, and M. Rotenberg (Academic Press, New York 1976, 16, pp. 327-365.

18. J.A. Bradshaw, in "Crossed-Field Microwave Devices", edited by E. Okress (Academic, New York, 1961), Vol. 1, p. 261, plus references therein.

19. J.M. Osepchuk, in "Crossed-Field Microwave Devices", edited by E. Okress (Academic, New York, 1961), Vol. 1, p. 275, plus references therein.

20. T.J. Orzechowski and G. Bekefi, Phys. Fluids 22, 978 (1979).

21. E.J. Baranchikov, A.V. Gordeev, V.D. Korolev, and V.P. Smirnov, Proc. Second International Topical Conference on High Power Electron and Ion Beam Research and Technology, Cornell University, Ithaca, N.Y. 1977, Vol. 1, p. 3.

22. S.P. Yu, G.P. Kooyers, and O. Buneman, J. Appl. Phys. 36, 2550, (1965).

23. G.D. Sims, in "Crossed-Field Microwave Devices", edited by E. Okress (Academic, New York, 1961), Vol. 1, p. 179.

24. J.A. Bradshaw, "Proceedings of the Symposium on Electronic Waveguides", Polytechnique Institute of Brooklyn (1958).

25. H. Nedderman, J. Appl. Phys. 26, 1420 (1955).

26. C.W. Hartman, University of California, Electronics Research Laboratory Report No. 10 (1960).

27. E. Ott and R.V. Lovelace, Appl. Phys. Lett. 27, 378 (1975).

28. O. Buneman, in "Crossed-Field Microwave Devices", edited by E. Okress (Academic, New York, 1961), Vol. 1, p. 209.

29. L. Brillouin, Phys. Rev. 60, 385 (1941); 62, 166 (1942); 63, 127 (1943); L. Brillouin and F. Block, Adv. Electron 3, 85 (1951); 3, 145 (1951).

30. O. Buneman, Nature 165, 474 (1950); J. Electron. Control 3, 1 (1957); 3, 507 (1957); C.V.D. Rept. Mag. 10, 11, 17, 30 (1943).

31. B.C. DePackh, Naval Research Laboratory Radiation Project Report No. 5 (1968); also Report No. 17 (1969).

32. E. Ott and R.V. Lovelace, Appl. Phys. Lett. 27, 378 (1975).

33. J.M. Creedon, J. Appl. Phys. 46, 2946 (1975); 48, 1070 (1977).

34. K.D. Bergeron, Phys. Fluids 20, 688 (1977).

35. D.R. Hartree, C.V.D. Rept. Mag. 1 (1941).

36. J. Slater, "Microwave Electronics" (Van Nostrand, New York, (1950).

37. D. Gabor, Proc. R. Soc., London Ser. A183, 436 (1945); D.

Gabor and G.D. Sims, J. Electron. 1, 25 (1955).

38. R.N. Sudan and R.V. Lovelace, Phys. Rev. Lett. 31, 1174 (1973).

39. R.V. Lovelace and E. Ott, Phys. Fluids 17, 1263 (1974).

40. A. Ron, A.A. Mondelli, and N. Rostoker, IEEE Trans. Plasma Sci. PS-1, 85 (1973).

41. A. Palevsky and G. Bekefi, Proc. IEEE International Conference on Plasma Science, University of Wisconsin, Madison (1980)p 94.

42. J.P. Quintenz and J.W. Poukey, J. Appl. Phys. 48, 2286 (1977).

43. H.R. Jory and A.W. Trivelpiece, J. Appl. Phys. 40, 3924 (1969).

44. A. Palevsky, Ph.D. Thesis (1980), Department of Physics, Massachusetts Institute of Technology.

FIGURE CAPTIONS

Fig. 1. Particle positions in the cathode-anode gap of a linear magnetron[9] 5ns and 15ns after applying the external voltage. The anode block is shown shaded. A dc magnetic field of 0.172T is perpendicular to the page.

Fig. 2. Distribution of particle momenta resolved parallel to the cathode surface at 5ns and 15ns. The cathode is at position zero meters. The anode is at 1.97×10^{-2}m and the top of the resonator vanes is at 4.50×10^{-2}m.

Fig. 3. The temporal development of the magnetron current, voltage and rf magnetic field. The field is measured inside a vane resonator and its amplitude is in relative units.

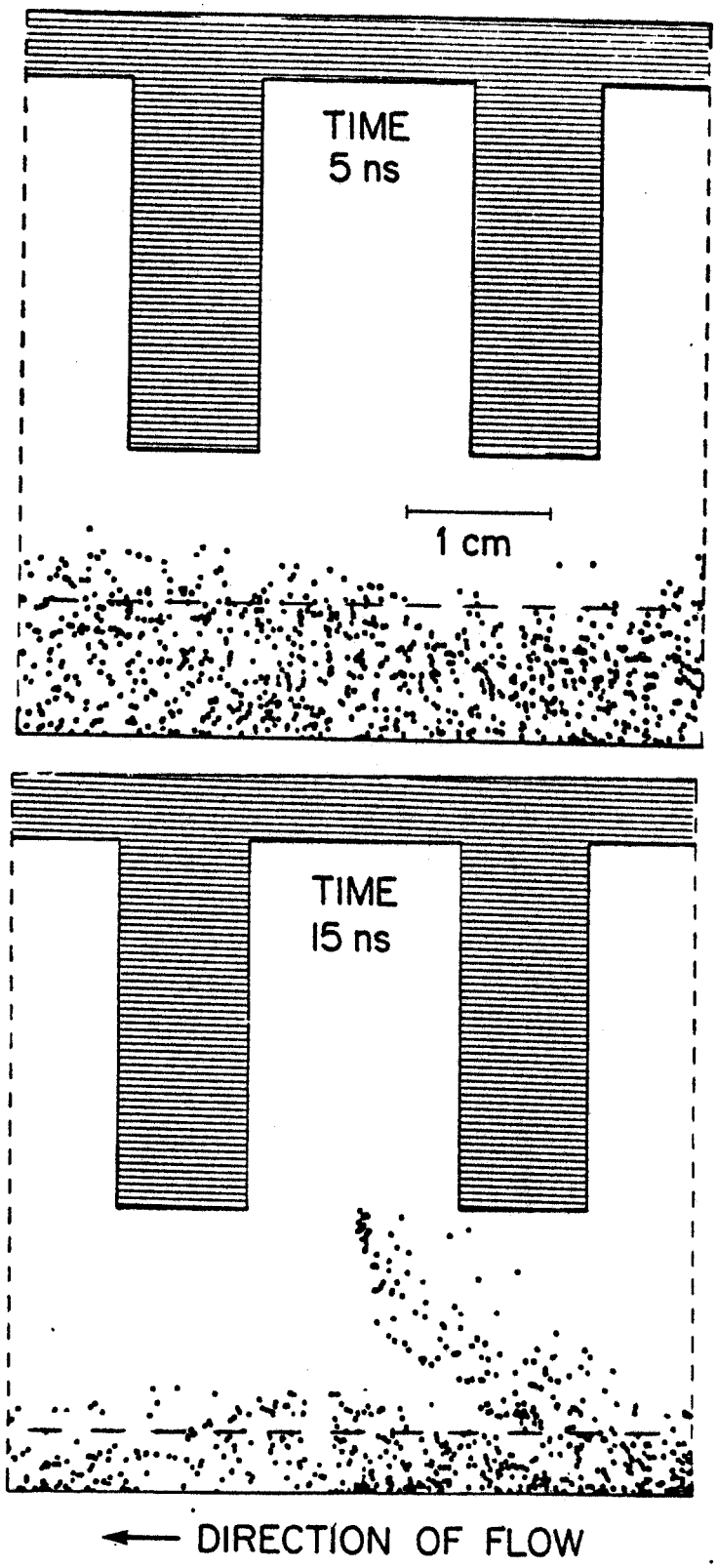

Fig. 1
Palevsky, Bekefi, & Drobot

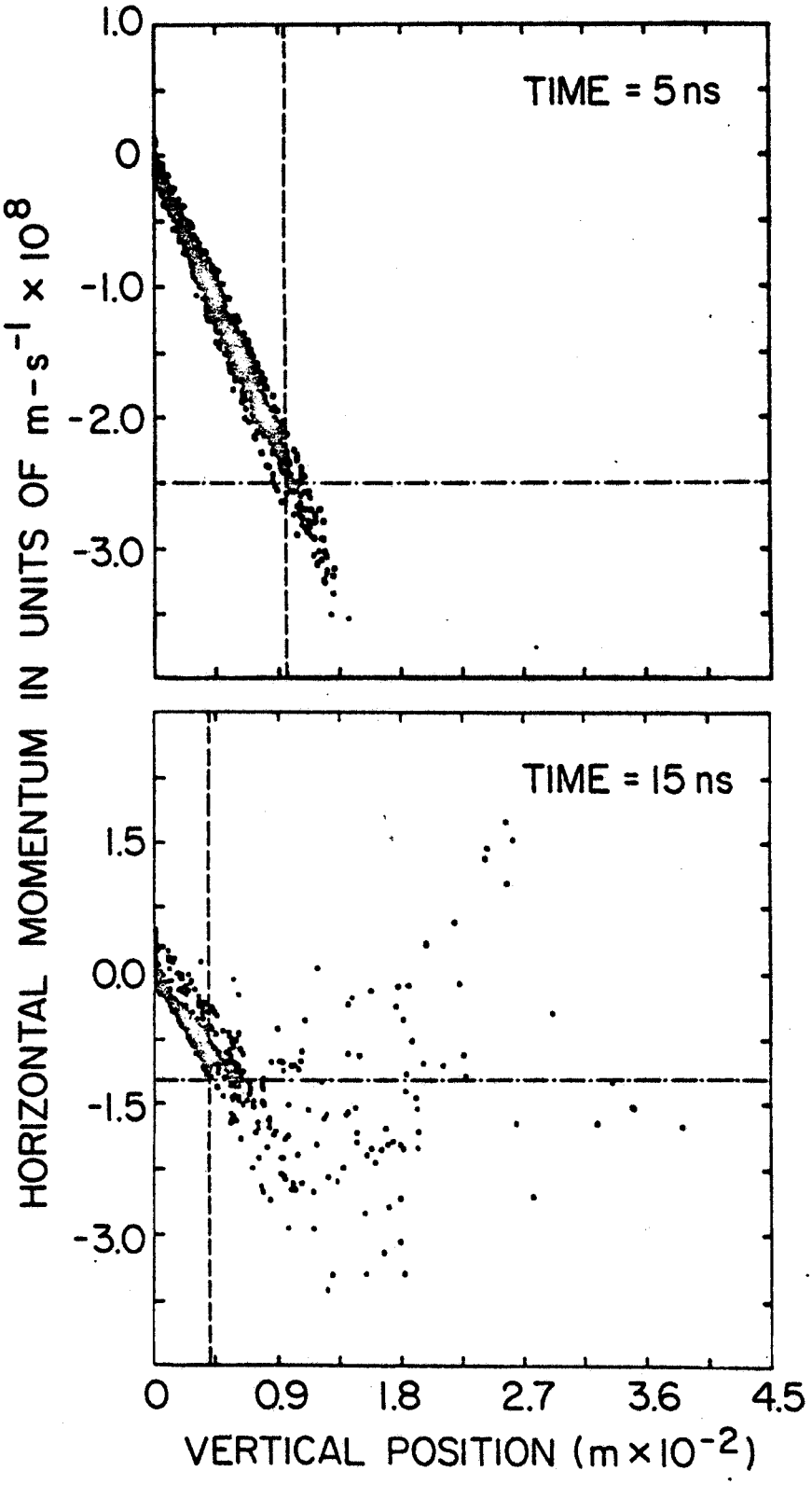

Fig. 2
Palevsky, Bekefi, & Drobot

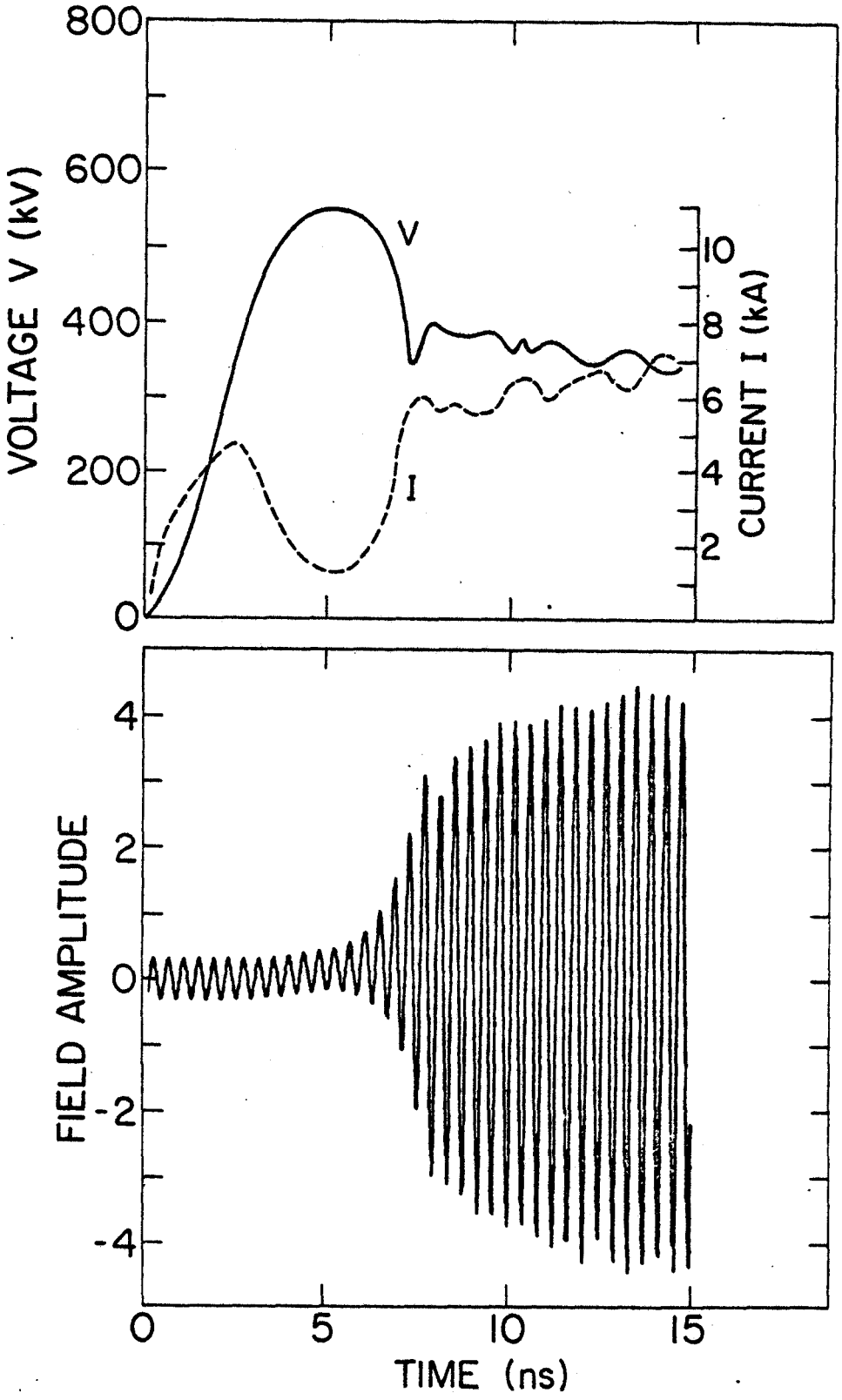

Fig. 3
Palevsky, Bekefi, & Drobot